Applied Catalysis B: Environmental 330 (2023) 122568

Contents lists available at ScienceDirect

Applied Catalysis B: Environmental

journal homepage: www.elsevier.com/locate/apcatb

Mechanistic study of water–gas shift reaction over copper/zinc-oxide/alumina catalyst in a reformed gas atmosphere: Influence of hydrogen on reaction rate

Keita Taniya [a,b,c,*], Yasuhiro Horie [a], Ryo Fujita [a], Yuichi Ichihashi [a,b,c], Satoru Nishiyama [a,b]

[a] Department of Chemical Science and Engineering, Graduate School of Engineering, Kobe University, Rokkodai, Nada, Kobe 657-8501, Japan
[b] Social Implementation of Renewable Energy Research Center, Graduate School of Engineering, Kobe University, Rokkodai, Nada, Kobe 657-8501, Japan
[c] Research Center for Membrane and Film Technology, Kobe University, Rokkodai, Nada, Kobe 657-8501, Japan

ARTICLE INFO

Keywords:
Water–gas shift reaction
Low-temperature shift
Cu-ZnO-Al_2O_3
Competitive redox mechanism
Active site estimation

ABSTRACT

Kinetic and pulse experiments were performed to elucidate the mechanism of the water–gas shift reaction (WGSR) under practical conditions. CO conversion was found to be significantly influenced by H_2. The reaction was strongly suppressed at high H_2 concentrations. A simple rate equation based on a competitive redox mechanism was derived. The H_2O-induced oxidation of Cu^0 to Cu^+ was assumed to be the rate-determining step. H_2 affected the CO conversion rate because it competitively reduced Cu^+ to Cu^0. In the proposed rate equation, the rate constant k_f determines the rate of the catalytic cycle and the selectivity factor κ may control the selectivity to CO conversion. CO-pulse experiments independently yielded the selectivity factor κ (1.38), which was almost identical to that obtained from the kinetic analysis (1.39). The coincidence of these values strongly corroborates the proposed competitive redox mechanism.

1. Introduction

The water–gas shift reaction (WGSR) is important in hydrogen production processes for enriching H_2. Moreover, it is crucial for decreasing the CO concentration in reformed gas, a mixture of CO, CO_2, H_2O, and H_2, to prevent the poisonous adsorption of CO onto the Pt active sites in fuel cells equipped with polymer electrolyte membranes.

Owing to the high activity and selectivity of copper for the WGSR, Cu-based catalysts are frequently employed for this reaction at low temperatures and CO concentrations. Since the early 1960s, ternary Cu-ZnO-Al_2O_3 (CZA) catalysts have been industrially used for the WGSR [1,2].

The WGSR, one of the slowest reactions in the chemical industry, is typically conducted at reaction temperatures and space velocities of 453–503 K and 1000–5000 h^{-1}, respectively; the preceding steam-reforming of methane is several tens of times faster than the WGSR. Consequently, hydrogen production processes require significantly large reactors for WGSR to satisfactorily reduce CO in the reformed gas, which is produced at high velocities. Therefore, faster catalytic systems with Cu-based catalysts should be studied at low reaction temperatures to overcome the equilibrium limitation of the WGSR [3].

Acquiring mechanistic information for specific reactions can considerably facilitate the development of highly active catalysts. Effective, focused approaches can be adopted to enhance the rate-limiting step of the reaction. Numerous mechanistic studies, including kinetic investigations, have been conducted to elucidate the mechanism of the WGSR [4]. For instance, Byron Smith et al. comprehensively reviewed the kinetics of the WGSR [4]. Unfortunately, definite and/or conclusive kinetic expressions and mechanisms have not yet been proposed for the WGSR. In general, the WGSR is believed to occur via two main reaction mechanisms: the associated (surface reaction) [4–9] and regeneration (redox) mechanisms [3,4,10–18]. The redox mechanism is considered to be dominant in high-temperature shift reactions over Fe-based metal oxide catalysts [4]. However, both the surface reaction and redox mechanisms have been considered for explaining the low-temperature shift reaction over Cu-based catalysts. Conflicting

Abbreviations: WGSR, water–gas shift reaction; CZA, Cu-ZnO-Al_2O_3; XRD, X-ray diffraction; XRF, X-ray fluorescence; XPS, X-ray photoelectron spectroscopy; AES, Auger electron spectroscopy; GC, gas chromatography; TCD, thermal conductivity detection; TOF, turnover frequency.

* Corresponding author at: Department of Chemical Science and Engineering, Graduate School of Engineering, Kobe University, Rokkodai, Nada, Kobe 657-8501, Japan.
E-mail address: taniya@platinum.kobe-u.ac.jp (K. Taniya).

https://doi.org/10.1016/j.apcatb.2023.122568
Received 28 October 2022; Received in revised form 23 February 2023; Accepted 2 March 2023
Available online 7 March 2023

experimental data is routinely generated in this regard. The problems encountered in this context are summarized below.

(1) Several rate expressions have been proposed based on both mechanistic hypotheses and theoretical–experimental fittings [4]. However, an appropriate rate equation that satisfies a wide range of reaction-gas atmospheres has not been reported. In practical settings, the reformed gas, which is the reactant gas for the WGSR, typically comprises CO and H_2O, as well as CO_2 and abundant H_2, because the WGSR is employed for the post-treatment of the reformed gas. The H_2 affects the rate and can determine the rate-limiting step in the WGSR occurring via the redox mechanism. This significant detrimental effect of H_2 is usually explained by a reverse WGSR; however, this reverse reaction is not dominant at low reaction temperatures, such as 453 K, because of the high equilibrium constant of the forward WGSR. The negative order with respect to H_2 may be explained by competitive adsorption over the active sites and the formation of spectator species such as formate; considering the former scenario, strong adsorption of H_2 is not expected to occur on Cu^0 surfaces, whereas with respect to the latter, details have been provided in the following paragraph.

(2) Surface intermediate species such as *formate*, *carbonate*, and *carboxylate*, which have been observed on Cu and/or ZnO sites by infrared spectroscopy, have been proposed to exist based on the surface reaction mechanism [19]. However, direct evidence has not been obtained in terms of determining the species that function as intrinsic intermediates. The observed surface adsorbates are believed to possibly function as *spectators* in the reaction [19,20]. Through DFT calculations, Gokhale et al. determined that the carboxyl surface species (COOH) on Cu-based catalysts could behave as an intermediate in the WGSR [19]. Additionally, the DFT-calculated overall barrier of the COOH intermediate formation was found to be smaller than that for $CO+O \rightarrow CO_2$ over Cu(111), indicating that the surface redox mechanism does not play a significant role in the WGSR [19]. Kalamaras et al. conducted steady-state isotopic transient kinetic analysis (SSITKA)-diffuse reflectance Fourier transform infrared spectroscopy (DRIFTS) experiments and determined that the formate and carbonate species on Pt/TiO_2 catalysts were stable and inactive spectators [20]. This suggests the presence of stable surface species that can be observed by IR spectroscopy; however, certain species do not function as reaction intermediates.

(3) With respect to the redox mechanism, the pressure dependence cannot explain why the rate equation includes the pressure-dependent terms of both CO (reductant) and H_2O (oxidant) in the case of rate-limiting oxidation or reduction. Moreover, the significant adverse effect of H_2 cannot be explained satisfactorily. Koryabkina et al. also reported a negative effect of H_2 on the WGSR [21].

A reasonable, rational reaction mechanism and rate expression are desired for the low-temperature WGSR over Cu-based catalysts conducted under practical reaction conditions. Therefore, the pressure dependence in the WGSR conducted over CZA catalysts in oxidizing and reducing atmospheres with CO and H_2O reactants was investigated in this study, and the observed dependence was compared with that obtained with a realistic gas composition. Moreover, competitive pulse experiments were conducted to derive a reasonable rate expression and a rational mechanism. The reaction pathway is discussed based on the redox mechanism, and an attempt is made to explain the low activity of the WGSR under practical reaction conditions. Additionally, a protocol is provided for estimating the number of active sites on the CZA catalysts used for low-temperature WGSR, in addition to a method for evaluating the surface Cu^0 atoms based on N_2O titration measurements.

2. Experimental

2.1. Catalyst preparation

Reagents used in this study were purchased from Nacalai Tesque (Kyoto, Japan). First, the CZA catalysts were prepared using a co-precipitation method. To this end, an aqueous sodium carbonate (Na_2CO_3) solution (1 M) was added dropwise to a mixed aqueous solution of $Cu(NO_3)_2{\cdot}3H_2O$, $Zn(NO_3)_2{\cdot}6H_2O$, and $Al(NO_3)_3{\cdot}9H_2O$. The metal reagents (total amount = 0.2 mol) were dissolved in deionized water (250 mL). The Na_2CO_3 solution (1 M) was added at a rate of 3.6 mL/min. The resulting solution was aged for 0.5 h after its pH reached 7, and the obtained precipitate was filtered and rinsed with hot deionized water (~ 343 K). The resulting precipitate was dried at 393 K for 24 h and then calcined in a flowing gas mixture of N_2 and O_2 (N_2:O_2 = 4:1) at 773 K for 3 h. The particle size of the calcined precipitate was controlled between 150 and 250 μm.

2.2. Activity tests

The WGSR was performed in a stainless-steel tubular flow reactor (ø 9.4 mm) under atmospheric pressure. Immediately before the reaction, the CZA precursor (0.5 g) was reduced in the reactor using a flowing gas mixture of H_2 and N_2 (H_2: 20 %) at 493 K for 2 h. H_2 was purged with N_2, and the temperature was lowered to the reaction temperature of 453 K. The gas flow (N_2) was then switched to the reactant gas. The standard composition of the reactant gas mixture ($CO/CO_2/H_2O/H_2$) for the catalyst activity evaluation was 10:5:30:55, which is almost identical to that of the effluent from the typical steam reforming of naphtha. The space velocity was 10,000 mL/h g-cat.

The pressure dependence of the rate of CO conversion was investigated based on the partial pressure of CO or H_2O at 453 K in a gas mixture of CO, H_2O, and N_2 (balance) at low conversions for operation under differential-reactor conditions. The space velocity was increased to 144,000 mL/h g-cat to limit the CO conversion to less than 20 %. The pressure-dependence experiments were conducted in H_2O-rich (oxidizing) and CO-rich (reducing) atmospheres. The reaction conditions used in this study are listed in Table 1. The composition of the product gas was analyzed by gas chromatography (GC).

The CO conversion (x) is estimated as follows:

$$x(\%) = \frac{F_{CO\bullet in} - F_{CO\bullet out}}{F_{CO\bullet in}} \times 100$$

where $F_{CO\bullet in}$ and $F_{CO\bullet out}$ are the molar feed rates of CO (mol/h) at the inlet and outlet of the reactor, respectively.

The experimentally measured reaction rate, $(-r_{CO})$, is evaluated as follows:

$$(-r_{CO})\left(\mathrm{mol}\Big/\mathrm{h}\bullet\mathrm{g}-\mathrm{cat}\right) = \frac{xF_{CO\bullet in}}{W}$$

where W is the catalyst weight (g-cat).

Table 1
Reaction conditions for evaluating the pressure dependence of CO and H_2O.

Condition	Run #	Constant components and pressures	
Oxidative	1	H_2O: 30.4 kPa	8.4 < CO < 13.5 kPa
	2	CO: 10.1 kPa	26.2 < H_2O < 32.5 kPa
Reductive	3	H_2O: 6.3 kPa	12.7 < CO < 15.8 kPa
	4	CO: 13.7 kPa	2.1 < H_2O < 8.4 kPa
Reforming	5	H_2O: 25.1 kPa CO_2: 6.0 kPa H_2: 46.0 kPa	6.0 < CO < 13.1 kPa
	6	CO: 8.4 kPa CO_2: 6.0 kPa H_2: 46.0 kPa	16.7 < H_2O < 29.3 kPa

The turnover frequency (TOF) is obtained as follows:

$$TOF\left(s^{-1}\right) = \left(-r_{CO}\right) \times \frac{1}{S_{Cu}}$$

where S_{Cu} is the surface amount of Cu^0 per gram of catalysts, as evaluated via N_2O titration.

2.3. Characterization

2.3.1. X-ray diffraction (XRD) analysis

Powder XRD patterns were obtained using a diffractometer (RINT 2100, Rigaku Co., Takatsuki) to determine the state of each component of the catalyst. The X-ray tube with a Cu target was operated at 40 kV and 20 mA.

2.3.2. High-angle annular dark-field scanning transmission electron microscopy (HAADF-STEM) and energy-dispersive X-ray spectroscopy (EDX)

HAADF-STEM images of CZA catalysts were obtained using JEM-2100F (JEOL, Japan) operated at an accelerating voltage of 200 kV. Elemental mapping via EDX was acquired using JED-2300T (JEOL, Japan), which was installed in the same TEM instrument.

2.3.3. X-ray fluorescence (XRF) spectroscopy

The composition of the co-precipitated catalyst was determined using an XRF spectrometer (Primini, Rigaku Co., Takatsuki) equipped with a Pd-Kα X-ray tube operated at 40 kV and 1.25 mA.

2.3.4. X-ray photoelectron spectroscopy (XPS) and Auger electron spectroscopy (AES)

The oxidation state of Cu in the CZA catalyst was determined by XPS and AES (PHI X-tool, ULVAC-PHI, Inc., Chigasaki) at the Center for Supports to Research and Education Activities, Kobe University. Al-Kα radiation (1486.6 eV) was used for excitation, and the X-ray tube was operated at 100 W. The binding energy of Cu2p was calibrated based on the C1s peak at 284.6 eV. Data processing was performed using Multi-Pak software (ULVAC-PHI, Inc.).

The samples subjected to different pretreatments were immediately transferred to the experimental apparatus to limit their exposure to air and consequently avoid the surface oxidation of the Cu species. Additionally, to reduce the effect of oxide species formed on the surface of Cu particles upon exposure to air, Ar-ion sputtering was performed at 1 kV for 60 s for all samples, except for the calcined specimen. A sputtering depth of 1.42 nm was used for SiO_2. The sputtering conditions were determined by the sputtering time at which Cu^+ species were hardly observed over the CZA catalyst, which was reduced using a flowing gas mixture of H_2 and N_2 (H_2: 20 %) at 493 K for 2 h.

2.3.5. N_2O titration

Surface Cu^0 atoms were titrated with N_2O to evaluate the surface area of Cu^0 using a BELCAT 40 instrument (MicrotracBEL, Osaka; formerly BEL Japan) at 323 K. The number of the surface Cu^0 atoms was evaluated using the following stoichiometry:

$$N_2O + 2Cu^0 \rightarrow Cu_2^+O + N_2.$$

The evolved N_2 was analyzed using a GC setup equipped with a thermal conductivity detection (TCD) instrument.

2.3.6. Successive and competitive pulse reaction

The competitive pulse reaction was conducted in a tubular flow reactor directly connected to a GC setup. The catalyst was reduced in a flowing H_2/N_2 gas mixture ($H_2/N_2 = 1/4$) at 493 K for 1 h, and the temperature was subsequently lowered to 453 K under flowing Ar. The relevant reaction conditions are listed in Table 2. Water was introduced through an evaporator attached to the inlet of the reactor using a microsyringe, and the CO/H_2 mixture was successively pulsed through a six-port sampling valve. Initially, several H_2O pulses were introduced until the H_2 evolution was complete. Subsequently, pulses of mixed CO and H_2 were introduced until the consumption of each gas stopped. The consumption of CO and H_2 was monitored by GC-TCD. The H_2O formed during the supply of the mixed pulse was trapped at 273 K immediately before the inlet of the GC device.

Table 2
Reaction conditions for successive pulse experiments.

a) Pulse characteristics	
Catalyst weight (mg)	50
H_2O pulse (μmol)[a]	11.1
Co-pulse	
CO (μmol)	1.3
H_2 (μmol)	1.4
b) ($CO + H_2$) mixed pulse characteristics	
Partial pressure of CO (kPa)	16.2
Partial pressure of H_2 (kPa)	17.7
Partial pressure of Ar (kPa)	67.4
Pulse size (mL)	0.200

[a] 0.2 μL of water.

3. Results and discussion

XRD patterns of the CZA catalyst after the H_2 reduction and WGSR with the reformed gas were acquired (Fig. 1). Peaks at $2\theta = 43.3°$ and 50.4° were attributed to metallic Cu (Crystallography Open Database (COD) No. 7101264), whereas those at 31.7°, 34.4°, 36.2°, 47.5°, and 56.5° were ascribed to ZnO (COD No. 9004179). Metallic Cu and ZnO were confirmed to be present on the catalyst in both scenarios, suggesting that the bulk structure of Cu metal in the CZA catalyst was hardly changed by the WGSR.

The HAADF-STEM image and EDX mapping of Cu, Zn, and Al (Fig. S1) clearly reveal that Cu, Zn, and Al are uniformly dispersed within a single particle of CZA catalysts, which are prepared via co-precipitation.

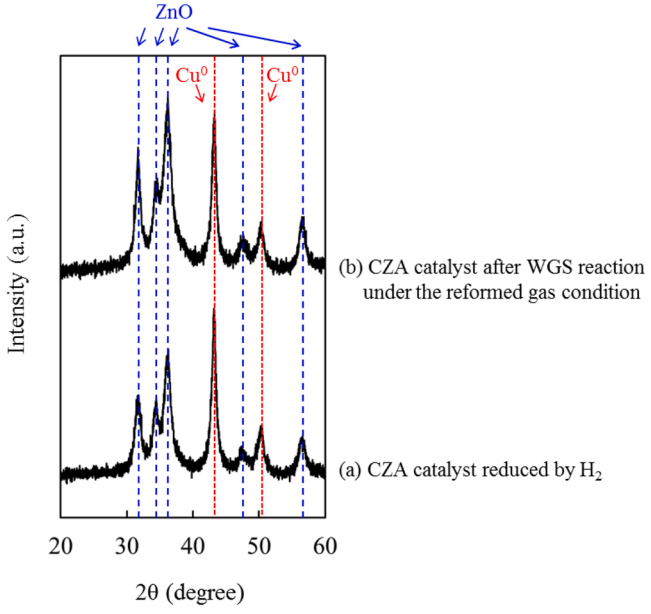

Fig. 1. XRD patterns of the CZA catalyst (a) reduced by H_2 prior to the WGSR and (b) after the WGSR under reformed gas conditions at 453 K for 4 h.

3.1. Pressure dependence on activity for WGSR

The catalytic activity for the WGSR is considerably affected by the gas composition. The variations in activity observed in this study are listed in Table 3. Runs 1–3 in Table 3 represent activities obtained when the reactant gas composition was similar to that of the effluent from the typical steam reforming of naphtha. CO conversion at 453 K was 56.0 % for a gas composition ($CO/CO_2/H_2O/H_2/N_2$) of 10:5:30:55:0 and a space velocity of 10,000 mL/h g-cat. Because the CO conversion had to be less than 20% for the kinetic measurements, the space velocity was changed to 50,580 mL/h g-cat. This level of CO conversion was achieved in Run 4 with a similar gas composition. When the gas was changed from the reformed gas to a mixture of only CO and H_2O, the CO conversion increased threefold from 11.9 % to 30.1 % (Runs 4 and 5, respectively; Table 3). Thus, the presence of H_2 and CO_2 in the reactant gas strongly suppressed the catalytic activity. The reformed gas contained a high concentration of H_2, and the detrimental effects of H_2 were particularly examined in this study. However, the detrimental effects of CO_2 were not considered.

3.1.1. H_2O-rich atmosphere (oxidizing conditions)

The CO conversion was suppressed to below 20 % to investigate the pressure dependence of the WGSR rate. The apparent reaction orders for CO and H_2O were estimated without co-feeding the CO_2 and H_2 products (Figs. 2 and 3). Notably, the estimated apparent reaction orders differed from those obtained by co-feeding the products (Figs. 2 and 3). The dependence of the reaction orders on the various conditions for the WGSR is discussed in this section. The dependence of the CO and H_2O partial pressures under oxidizing conditions was studied (Runs 1 and 2 in Table 1). Fig. 2 shows double logarithmic plots featuring the partial pressures of CO and H_2O without H_2 and CO_2 in the reactant gas. The H_2O and CO partial pressures exhibited an almost zero order (Fig. 2**b**) and a significant positive order (Fig. 2**a**), respectively. These results suggest that the surface-active sites (Cu^0) were almost completely oxidized by H_2O, converted to Cu^+, and produced H_2 via the redox mechanism. The surface-active sites were fully oxidized under the oxidizing conditions. The rate-limiting step was presumably the reduction of Cu^+ to Cu^0, which produced CO_2. Oliveira et al. reported the zero-order dependence of H_2O for Cu/Al_2O_3 catalysts operated under H_2O-rich conditions [22] and suggested a redox mechanism for the WGSR. The surface reaction mechanism also suggests that the surface was fully covered with H_2O molecules, indicating a zero order for the H_2O partial pressure. No oxidized Cu species was observed after the reduced CZA catalysts were treated under a CO_2 stream at 453 K (Fig. S2), suggesting that CO_2 did not oxidize Cu^0 to Cu^+ at 453 K. In contrast, H_2 reduced Cu^+ to Cu^0 at 453 K. The produced H_2 possibly participated in the reduction of Cu^+, which could not be ignored even if the CO conversion was less than 20 %. The apparent reaction order for CO was underestimated.

3.1.2. CO-rich atmosphere (reducing conditions)

Fig. 3 shows the dependence on the CO and H_2O partial pressures, with a significant positive order observed for the latter. These results suggest that the rate-limiting step changed from reduction to the H_2O-induced oxidation of Cu^0 to Cu^+, which formed H_2 via the redox mechanism. Li et al. investigated the WGSR over Cu-Ce(La)O_x catalysts under CO-rich conditions [23] by considering the redox mechanism induced by CO and H_2O. The surface reaction mechanism can also explain the saturation of the surface-active sites with CO molecules.

Table 3
Effects of gas composition on the activity of the CZA catalyst[a] for the WGSR.

Run#	React. temp. (K)	Space velocity (mL/h g-cat)	Gas composition $CO:CO_2:H_2O:H_2:N_2$	CO conversion (%)
1	473	10,000	10:5:30:55:0	77.2
2	453	10,000	10:5:30:55:0	56.0
3	433	10,000	10:5:30:55:0	26.9
4	453	50,580	10.6:5.9:24.8:45.4:13.3	11.9
5	453	50,000	10:0:30:0:60	30.1

[a] The catalyst was prepared by co-precipitation; atomic ratios of Cu, Zn, and Al (50:43:7) were estimated by XRF.

3.1.3. Simulated reformed gas atmosphere

Fig. 4 shows the pressure dependences corresponding to Runs 5 and 6 (Table 1). Complicated dependences of the CO and H_2O partial pressures were observed. Although H_2O-rich reaction conditions were employed, the reaction atmosphere was considerably more reducing because of the high H_2 concentration. The dependence of the CO partial pressure was significant (Fig. 4**a**), resulting in a higher order (~ 0.7) than that derived from Fig. 2**a**. Moreover, the estimated reaction order for H_2O (~ 0.3; Fig. 4**b**) was greater than that obtained from Fig. 2**b**. Thus, higher reaction orders were obtained for both CO and H_2O under the reforming conditions. The complicated pressure dependence for the WGSR suggests that the presence of H_2 at high concentrations strongly affected the apparent CO conversion rate. Under the CO-rich conditions, only H_2O functioned as the oxidizing species in the reaction gas flow. CO_2 molecules could not have oxidized Cu^0 under these reaction conditions, even if CO_2 was formed in the reactor. The reaction order of H_2O (0.312; Fig. 4**b**) can be considered to be close to the intrinsic reaction order of H_2O.

Langmuir–Hinshelwood-type rate equations have frequently been proposed for the surface reaction mechanism. The negative terms in these equations have been considered in elucidating the competitive adsorption of the reactants (CO, H_2O) as well as products (CO_2, H_2) of the WGSR and/or the contribution of the reverse WGSR [4]. The typical rate equation is as follows:

$$(-r_{CO}) = \frac{kP_{CO}{}^{a}P_{H2O}{}^{b}}{\left(1 + K_{CO}P_{CO}{}^{a} + K_{H2O}P_{H2O}{}^{b} + K_{CO2}P_{CO2} + K_{H2}P_{H2}{}^{0.5}\right)^{2}}\cdot(1-\beta), \quad (1)$$

where β is a reverse reaction term that is expressed below (Eq. (2)).

$$\beta = \frac{P_{CO2}P_{H2}}{P_{CO}P_{H2O}}\frac{1}{K_{eq}}, \quad (2)$$

β approaches unity if the reaction conditions are close to equilibrium. β was calculated to be ~ 0.003 under the reaction conditions listed in Table 3, with the equilibrium constant at 453 K considered as 322 [4]. Additionally, the equilibrium conversion of CO in the reformed gas ($CO/CO_2/H_2O/H_2$ = 10/5/30/55) at 453 K was calculated as 98.8 %. This implies that the contribution of the reverse WGSR can be neglected under the experimental conditions employed in this study. Evidently, the reverse WGSR hardly proceeded over the CZA catalyst at 453 K in a gas mixture of CO_2, H_2, and N_2 ($CO_2/H_2/N_2$ = 5/55/40). The significant adverse effect of H_2 can be attributed to the strong adsorption of H_2 if the surface reaction mechanism is appropriate for the WGSR. However, H_2 molecules are not expected to strongly adsorb onto the metallic Cu or ZnO surfaces. The lower coverage of CO and H_2O than that of H_2 could explain the significant positive pressure dependence (Fig. 4) through a Langmuir–Hinshelwood mechanism. However, explaining the pressure-dependence behavior using a Langmuir–Hinshelwood-type reaction mechanism is difficult. Thus, the detrimental effect of H_2 on the activity for the WGSR had to be explained by another reason.

XPS profiles of $Cu2p_{3/2}$ on the CZA samples subjected to various treatments were acquired (Fig. 5). Only Cu^{2+} species were observed after the calcination of the catalyst precursor (spectrum [a] in Fig. 5). After the reduction, 4 h reaction, and H_2O treatment, Cu^0 or Cu^+ was observed on the CZA catalysts, as indicated in the $Cu2p_{3/2}$ XPS profiles ([b]–[d] in Fig. 5). The LMM Auger excitation spectra of Cu induced by Al Kα radiation are shown in Fig. 6. The results indicate that Cu^0 was the major surface component after the reduction of the catalyst precursor at

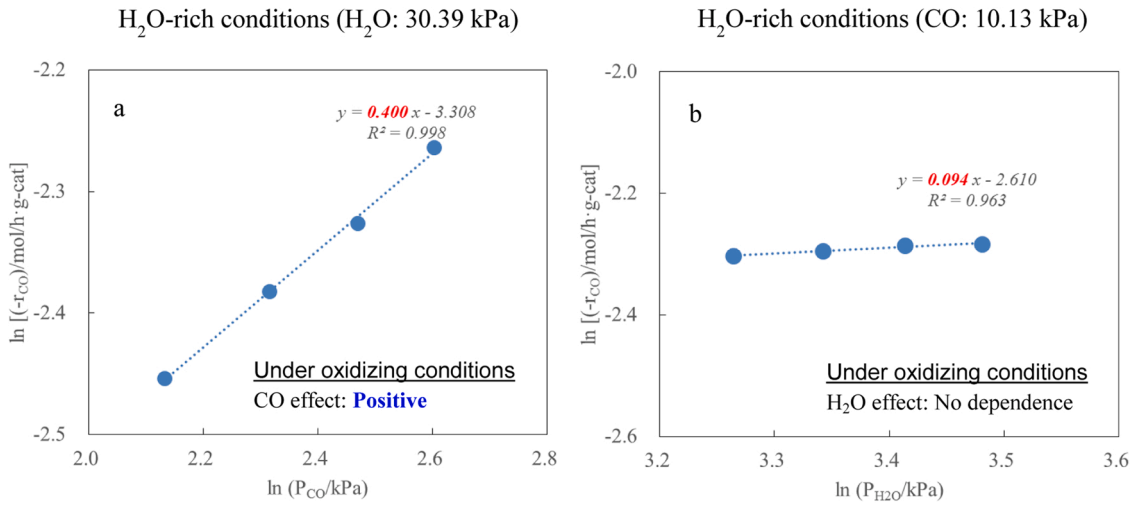

Fig. 2. Dependence of pressure on CO conversion rate under H_2O-rich conditions: dependence on (a) CO and (b) H_2O for Runs 1 and 2 (Table 1), respectively.

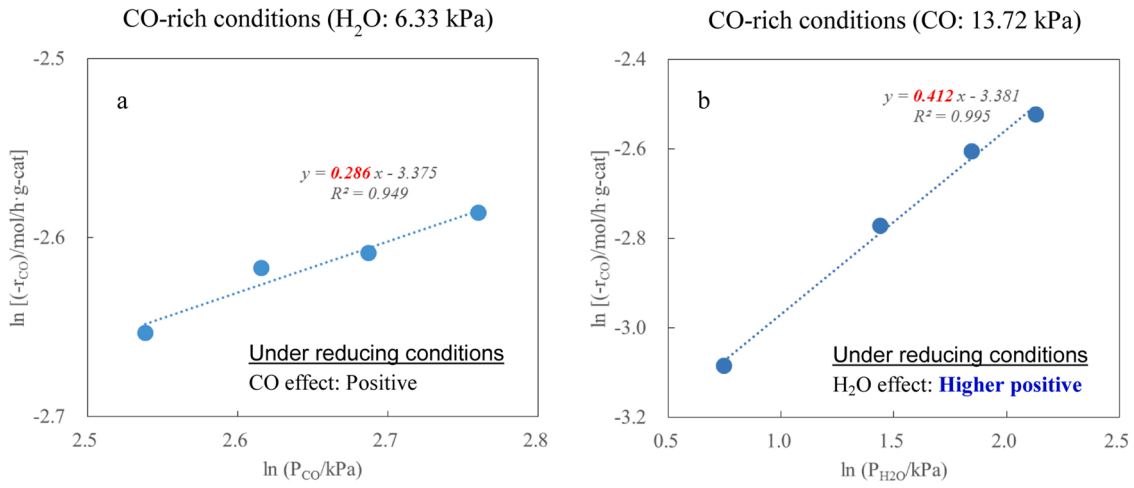

Fig. 3. Dependence of pressure on CO conversion rate under CO-rich conditions: dependence on (a) CO and (b) H_2O for Runs 3 and 4 (Table 1), respectively.

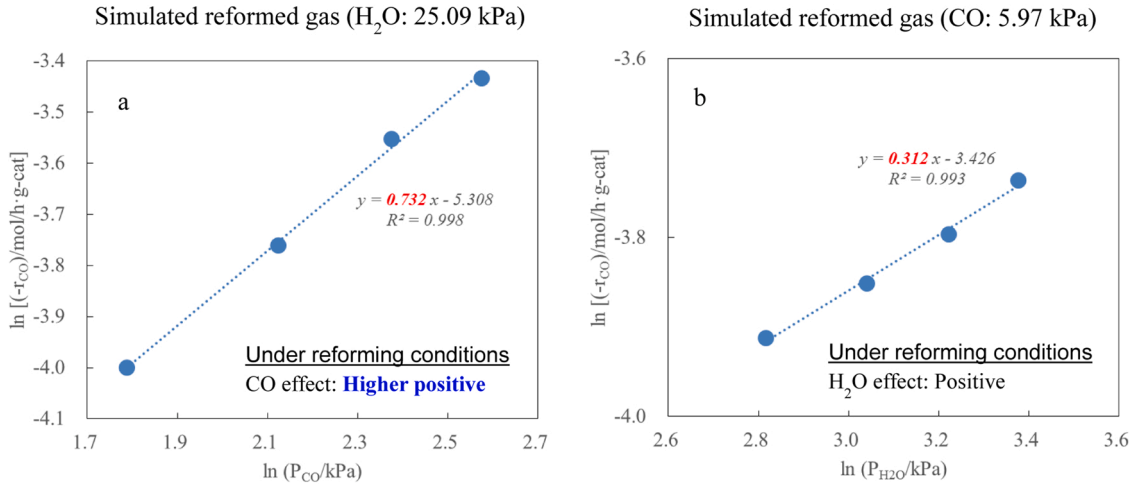

Fig. 4. Pressure dependence on CO conversion rate under reformed gas conditions: dependence on (a) CO and (b) H_2O for Runs 5 and 6 (Table 1), respectively.

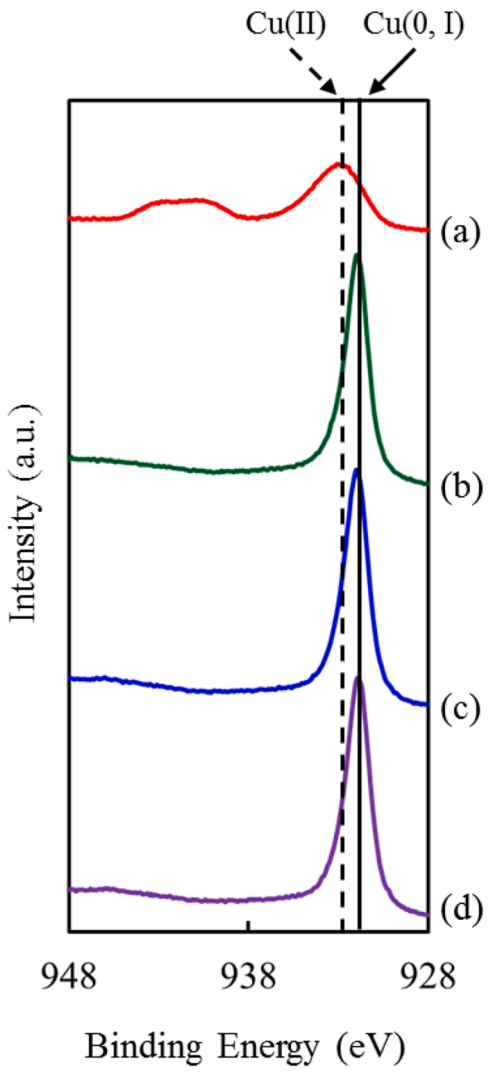

Fig. 5. XPS profiles acquired in the binding energy range of $Cu2p_{3/2}$ on CZA that underwent different treatments. (a) CZA precursor calcined in air and (b) subsequently subjected to H_2 reduction, (c) CZA catalyst after the WGSR at 453 K for 4 h, and (d) CZA catalyst reduced by H_2 and thereafter treated with H_2O at 453 K for 1 h. Ar-ion sputtering was conducted for 60 s for all samples, except for (a).

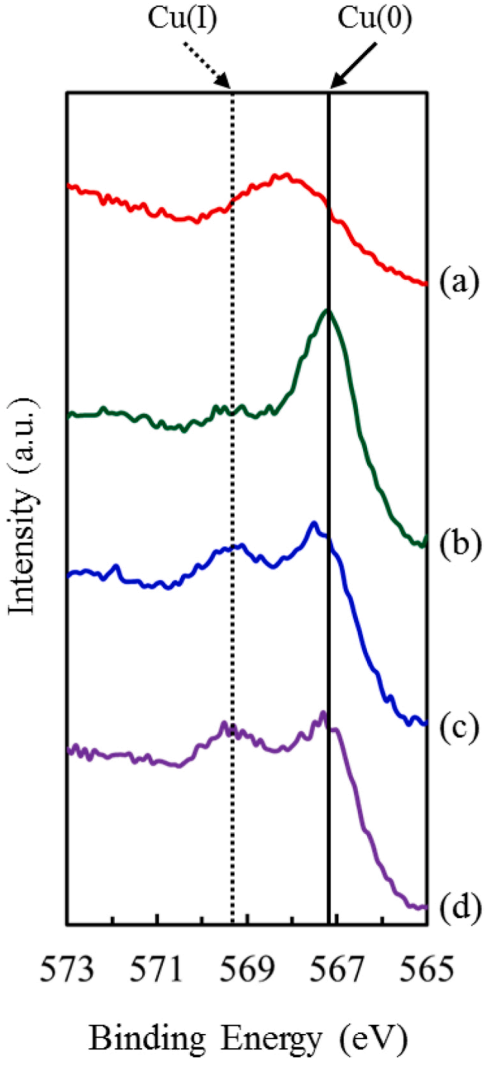

Fig. 6. Cu LMM Auger spectra of (a) CZA precursor calcined in air and subsequently (b) subjected to H_2 reduction, (c) CZA catalyst after the WGSR at 453 K for 4 h, and (d) CZA catalyst reduced by H_2 and thereafter treated with H_2O at 453 K for 1 h. Ar-ion sputtering was performed for 60 s for all samples, except for (a).

493 K (spectrum [b] in Fig. 6). A significant amount of Cu^+ was observed after 4 h of the reaction at 453 K (spectrum [c] in Fig. 6). Moreover, a similar spectrum was obtained after the H_2O treatment at 453 K for 1 h (spectrum [d] in Fig. 6). These results strongly suggest the occurrence of a redox cycle during the WGSR between Cu^0 and Cu^+, that is, the redox mechanism. Additionally, the XPS experiments confirmed that Cu^{2+} was not formed during the WGSR.

A simple redox mechanism cannot explain this complicated pressure dependence. Thus, the adverse effect of H_2 must be explained without the poisonous adsorption of H_2.

The CO conversion was estimated from the rate of the CO-induced reduction of Cu^+ to Cu^0, which formed CO_2 via the redox mechanism. If the WGSR over the CZA catalyst proceeded via the redox mechanism at ~ 453 K, the rate-limiting step had to be H_2O-induced oxidation because of the highly reducing nature of the reaction atmosphere (high-concentration H_2 in the reformed gas), although the partial pressures of H_2O were higher than those of CO (H_2O-rich conditions). The hydrogen in the reaction atmosphere likely played an important role in the reduction (or regeneration) of Cu^+ to Cu^0. Moreover, the reduction of Cu^+ was possibly enabled by H_2. In that scenario, H_2 reduced Cu^+ to Cu^0 without consuming CO (forming CO_2), which indicated that H_2 suppressed the CO conversion. The intrinsic turnover frequency (TOF) of the catalytic cycle for the WGSR was evidently the rate of the H_2O-induced oxidation of Cu^0 to Cu^+, according to the redox mechanism; however, the experimental activity was evaluated based on the CO conversion rate. When H_2 molecules participated in the reduction of Cu^+, the conversion of CO was strongly suppressed. In the surface reaction (associated) mechanism, this detrimental effect could be explained by the reverse WGSR. Unfortunately, the reverse WGSR was not significant at temperatures less than 473 K because of its low equilibrium constant (as opposed to a higher constant for the WGSR). However, the contribution of the reverse WGSR cannot be easily explained according to the surface reaction mechanism. Thus, the following hypotheses had to be tested: 1) the reaction proceeded via the redox mechanism; 2) H_2O-induced oxidation in the H_2-containing reaction gas atmosphere was assumed to be the rate-limiting step; and 3) H_2 molecules participated in the reduction of Cu^+ to Cu^0, with the reduction competing with the main WGSR route (CO and H_2). Successive pulse experiments were performed to comprehensively elucidate the redox behavior during the WGSR over the CZA catalyst.

3.2. Successive pulse experiments over CZA catalyst

Successive pulse experiments were performed under the conditions listed in Table 2. To this end, water vapor pulses were initially introduced until H_2 formation was terminated. Subsequently, pulses of a CO/H_2 gas mixture were introduced. The evolution of H_2 and consumption of CO and H_2 were investigated (Fig. 7). The first four pulses of H_2O resulted in H_2 evolution, and the consumption of CO and H_2 was observed during pulses of the CO/H_2 mixture (Fig. 7). Four pulse experiments were performed, and the results are summarized in Table 4. The amounts of H_2 formed and CO and H_2 consumed in Table 4 represent the total amounts recorded until no formation or consumption was observed. Run 4 in Table 4 corresponds to the calculated results shown in Fig. 7. The average H_2 evolution was 31.9 μmol/g-cat and the overall consumption of CO and H_2 was 30.5 μmol/g-cat, essentially indicating a balance between the reduction and oxidation. The pulse experiments represent the separate elementary steps of the WGSR occurring via the redox mechanism. The reduction of the oxidized Cu species was achieved mainly by CO, whereas the selectivity of the CO-enabled reduction—which is the main process in the WGSR occurring via the redox mechanism—was 0.737 (Table 5).

3.3. Rate equation based on the competitive redox mechanism

The following competitive redox mechanism was postulated based on the aforementioned findings:

Table 4
Formation of H_2 and consumption of CO or H_2 in the successive pulse experiments.

Run #	H_2O pulse[a]	(CO + H_2) mixed pulse[b]		(CO + H_2) consumption H_2 formation
	H_2 formation (μmol/g-cat)	CO consumption (μmol/g-cat)	H_2 consumption (μmol/g-cat)	
1	32.4	-	-	-
2	29.2	22.8	8.90	1.09
3	30.1	22.2	6.90	0.967
4	35.8	22.4	8.30	0.858
average	31.9	22.5	8.03	0.970

[a] Amount of H_2O introduced in one pulse: 220 μmol/g-cat.
[b] Amounts of CO and H_2 introduced in a mixed pulse: 26 and 28 μmol/g-cat, respectively.

Table 5
Selectivity of reduction in the WGSR and the estimated κ factors.

Reduction selectivity	
$CO/(CO + H_2)$	0.737
Ratio of reduction rate	
CO/H_2	2.80
Rate constant ratio κ	
κ estimated from reaction data	1.39
κ estimated from pulse experiment data	1.38

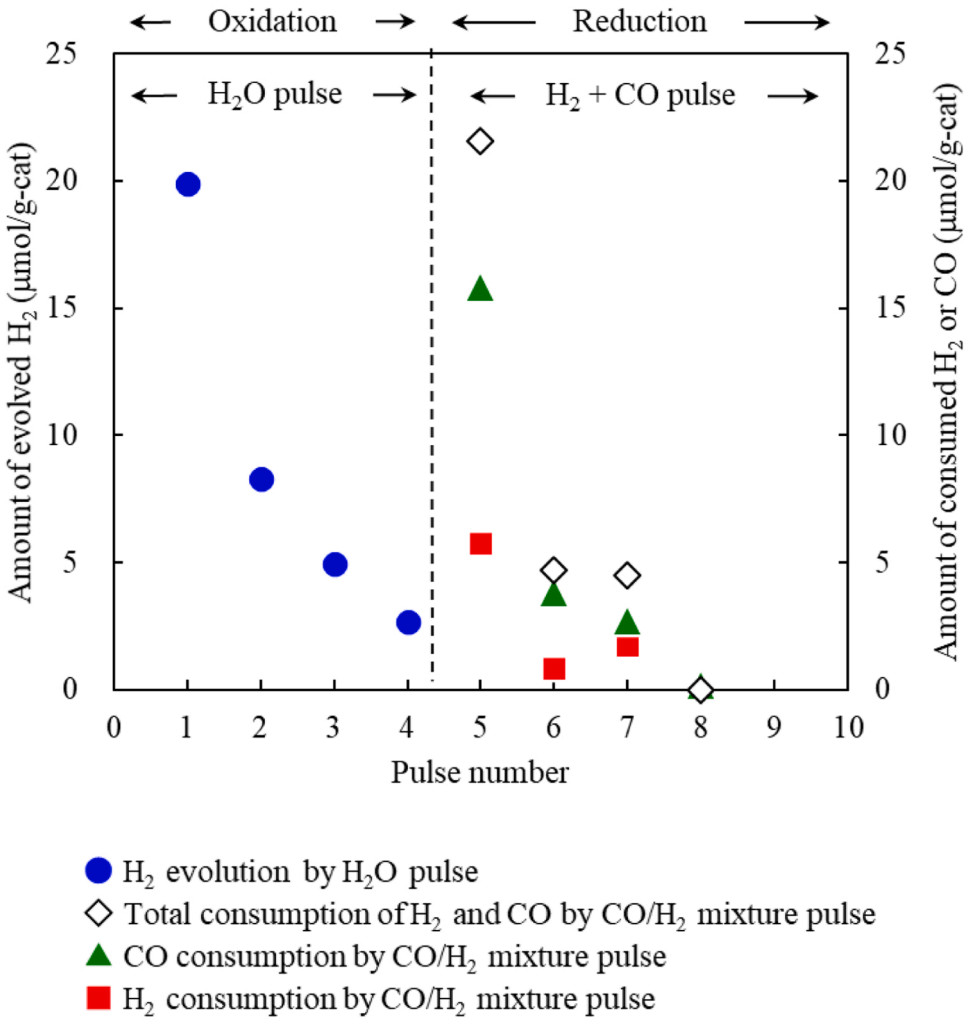

Fig. 7. A typical successive pulse experiment conducted at 453 K. The reaction conditions are summarized in Table 2.

1) The reaction proceeded via a catalytic cycle involving the H_2O-enabled oxidation of Cu^0 to Cu^+, followed by the CO- or H_2-induced reduction of Cu^+ to Cu^0.
2) H_2O-induced oxidation was assumed to be the rate-determining step. The turnover number of the catalytic cycle was determined by the rate of the H_2O-enabled oxidation. The oxidation was considerably slow, and the reaction atmosphere was highly reducing in nature.
3) The apparent reaction rate was significantly affected by the competitive reduction. The reduction of Cu^+ by H_2 (the reverse of the oxidation) did not contribute to the CO conversion. Therefore, the selectivity of CO-induced reduction was crucial for estimating the CO conversion rate.

The proposed reaction rate for CO conversion in the WGSR is expressed in Eq. (3).

$$(-r_{CO}) = k_f {P_{H2O}}^a \frac{k_{CO}{P_{CO}}^b}{k_{CO}{P_{CO}}^b + k_{H2}{P_{H2}}^c}, \quad (3)$$

where $k_f P_{H2O}^a$ represents the rate of the catalytic cycle, and the second term in Eq. (3) represents the selectivity of the reduction. Eq. (3) can be rearranged into Eq. (4), as follows:

$$(-r_{CO}) = k_f {P_{H2O}}^a \frac{1}{1 + \kappa\ ({P_{H2}}^c / {P_{CO}}^b)}, \quad (4)$$

where κ is the ratio of the rate constants k_{H2} and k_{CO} (k_{H2}/k_{CO}) in the competitive reduction process.

To clarify the adverse effect of H_2, the rate of the CO conversion reaction was measured under the conditions listed in Table 6. CO_2 was excluded from the reaction gas. The conversion of CO was less than 15 % at a space velocity of 144,000 mL/h g-cat (0.1 g of catalyst; flow rate of 240 mL/min) and a reaction temperature of 453 K. The parameters k_f and κ in Eq. (4) were optimized using the experimental data obtained under the conditions listed in Table 6. There was little ambiguity in the optimization. The reaction orders a, b, and c in Eq. (4) were optimized as 0.5, 1, and 0.5, respectively. The procedure adopted to estimate these parameters is thoroughly described in the SI. Eq. (4) can be rewritten as Eq. (5).

$$(-r_{CO}) = k_f {P_{H2O}}^{0.5} \frac{1}{1 + \kappa\ ({P_{H2}}^{0.5} / P_{CO})}, \quad (5)$$

Notably, Eq. (5) includes only two parameters.

This equation suggests that the oxidation proceeded via dissociative adsorption of H_2O, and the reduction induced by CO and H_2 could have occurred via associatively adsorbed CO and dissociatively adsorbed H_2. The rate constant k_f is the overall rate constant of the catalytic cycle, and κ is the ratio of the rate constants k_{H2} and k_{CO} in the competitive reduction process. Yeragi et al. proposed a redox-mechanism-based rate equation [24] and suggested that the H_2O-induced oxidation was rate-determining, considering the equilibrium with the CO-induced reduction. However, their equation could not explain the adverse effect of H_2.

The rate constant k_f and ratio κ in Eq. (5) were evaluated as 0.0292 mol/h g-cat $kPa^{0.5}$ and 1.39 $kPa^{0.5}$, respectively, at 453 K. The finally obtained rate equation at 453 K is shown in Eq. (6).

$$\left(-r_{CO}\right) = (0.0292)\cdot {P_{H2O}}^{0.5} \frac{1}{1 + (1.39)\cdot\ ({P_{H2}}^{0.5} / P_{CO})}\ [\mathrm{mol/h\cdot g - cat}] \quad (6)$$

A comparison between the experimental reaction rate calculated from the CO conversions and the estimated rate based on Eq. (6) is shown in Fig. 8. A good correlation was observed between the experimental data and estimated rates.

The selectivity of the reduction was estimated to be 0.737 from the pulse data listed in Table 6, and the ratio for the competitive reduction process $k_{CO}P_{CO}/k_{H2}P_{H2}^{0.5}$ can be expressed as:

Table 6
Reaction conditions for confirming the detrimental effect of H_2.

Run#	P_{CO} (kPa)	P_{H2O}	P_{H2}	P_{CO2}	CO conversion (%)	Observed CO conversion rate (mol/h g-cat)
1	12.7	6.3	0	0	8.8	0.070
	↓				↓	↓
	15.8				7.3	0.073
2	13.7	2.1	0	0	5.3	0.046
		↓			↓	↓
		8.4			9.2	0.080
3	16.9	4.2	42.2	0	4.2	0.045
			↓		↓	↓
			60.4		3.4	0.037
4	2.1	6.3	9.5	0	12.1	0.016
	↓				↓	↓
	5.3				9.5	0.032
5	6.9	2.1	6.9	0	7.4	0.032
		↓			↓	↓
		8.4			14.0	0.061
6	2.5	6.3	7.6	0	18.7	0.030
	↓		↓		↓	↓
	4.4		13.3		13.0	0.037
7	3.2	2.1	9.5	0	10.1	0.020
		↓			↓	↓
		8.4			18.4	0.037
8	6.3	6.3	6.3	0	13.1	0.053
	↓		↓		↓	↓
	7.9		7.9		11.0	0.055
9	4.2	12.7	16.9	0	14.3	0.038
			↓		↓	↓
			27.4		12.8	0.034

The space velocity was 144,000 mL/h g-cat.

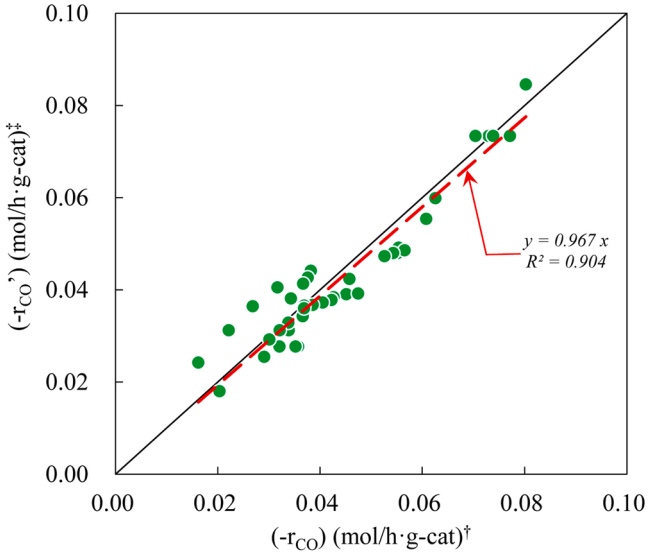

Fig. 8. Comparison of CO conversion rates determined experimentally and calculated based on the proposed reaction mechanism. The solid line is a visual guide representing calculated values identical to the experimental data. † Experimentally measured reaction rate under conditions leading to CO conversions of < 20 %. ‡ Estimated reaction rate for the WGSR over the CZA catalysts according to the following rate equation:

$$(-r'_{CO}) = 0.0292 P_{H2O}^{0.5} \frac{1}{1 + 1.39\left(P_{H2}^{0.5}/P_{CO}\right)}$$

$$\frac{k_{H2}}{k_{CO}}\frac{P_{H2}{}^{0.5}}{P_{CO}} = \left(\frac{k_{CO}P_{CO}}{k_{H2}P_{H2}{}^{0.5}}\right)^{-1} = \frac{k_{H2}P_{H2}{}^{0.5} + k_{CO}P_{CO}}{k_{CO}P_{CO}} - 1 = \frac{1}{(selectivity)} - 1 = \frac{1}{0.737} - 1 = 0.357$$

$$\frac{k_{CO}P_{CO}}{k_{H2}P_{H2}{}^{0.5}} = \frac{1}{0.357} = 2.80$$

The partial pressure data obtained in the pulse experiments are listed in Table 2; therefore, P_{H2} and P_{CO} values of 17.7 and 16.2 kPa, respectively, were substituted into the aforementioned equations, yielding.

$$\frac{k_{H2}}{k_{CO}}\frac{P_{H2}{}^{0.5}}{P_{CO}} = \frac{k_{H2}}{k_{CO}}\left(\frac{17.7^{0.5}}{16.2}\right) = \frac{1}{2.80}$$

$$\frac{k_{H2}}{k_{CO}} = \kappa = \frac{1}{2.80}\left(\frac{16.2}{17.7^{0.5}}\right) = 1.38$$

The parameter κ was evaluated using independently obtained data from both the kinetic analysis of the reaction rate data and pulse experiments. The independently estimated values of κ—1.39 and 1.38—are almost identical. These results strongly suggest that the proposed simple redox-based mechanism involving competitive reduction is appropriate. The selectivity, ratio of the reduction rate, and estimated values of κ are summarized in Table 5.

The catalytic cycle postulated in this study is illustrated in Scheme 1. Active Cu^0 sites react with H_2O to produce H_2, and two Cu^0 sites are oxidized to two Cu^+ ions. Oxidation is assumed to be the rate-determining step because of the significant reducing nature of the reaction atmosphere. Furthermore, oxidation by H_2O is assumed to be the rate-determining step because the bulk of Cu species remains Cu^0 after the WGSR is conducted in the reforming gas atmosphere (Figs. 1**b and** 6**c**).

When Cu^+ is reduced to Cu^0 (Scheme 1), the selectivity of the CO- or H_2-induced reduction of Cu^+ to Cu^0 strongly affects the apparent CO conversion in the reformed gas atmosphere. Hydrogen and carbon monoxide can completely reduce CuO to Cu [25–27]. Rodriguez et al. reported that CuO was reduced to Cu metal by hydrogen without the stable formation of Cu_2O even under mild reduction conditions such as at 210 °C under a 5 % H_2/95 % He mixture (flow rate = 1 mL/min) [26]. In contrast, according to Wang et al., CO can form Cu_2O as the primary product from CuO at 224 °C under a 5 % CO/95% He mixture (flow rate = 1 mL/min) [27]. Therefore, the reducing ability of H_2 is expected to be stronger than that of CO.

In terms of reducing ability, the Cu^+ reduction by H_2 appears to proceed preferentially compared with that by CO. However, the magnitude of the selectivity of CO-induced reduction (0.737 evaluated from the pulse data) indicates that the Cu^+ in the CZA catalyst is preferentially reduced by CO rather than by H_2. The strong affinity between Cu^+ and CO explains the high selectivity. A π complexation bond, which is considered stronger than van der Waals forces, is reported to form between Cu^+ and CO [28,29]. Yin et al. reported that Cu_2O-loaded SBA-15 adsorbents can selectively adsorb CO from the gas mixture of CO, H_2, and N_2 [29]. With reference to catalysts, significant irreversible adsorption of CO was also observed on the Cu^+ sites but not on Cu^0 and Cu^{2+}. Sarkany et al. reported that CO could more readily reduce Cu species in CuZSM-5 catalysts because of the strong interactions between CO and Cu^+ ions [30]. These results strongly suggest that the highly selective CO adsorption on Cu^+ in CZA catalysts, which are formed by H_2O-oxidation of Cu metal, preferentially facilitates the reduction of Cu^+ by CO; however, the reducing ability of CO is inferior to that of H_2. The selectivity of the reduction step reveals a crucial performance aspect of the WGSR catalyst.

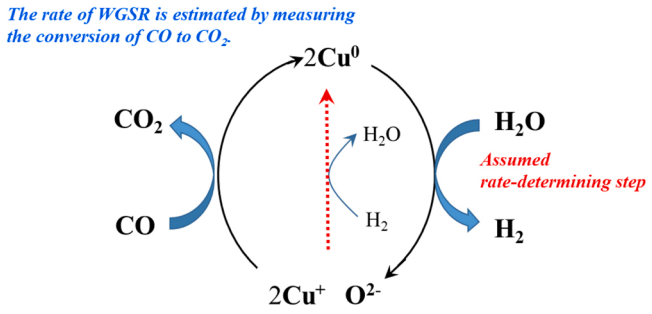

Scheme 1. Reaction pathway of WGSR over Cu-based catalysts under reductive atmosphere.

The rate constant k_f determines the intrinsic rate of the catalytic cycle for the WGSR, and the parameter κ—which is the selectivity factor of the reduction—controls the formation of CO_2. Considerable attention must be paid to both k_f and κ to understand the effects of catalyst-related factors, such as the composition (bulk and surface), particle size, mixing state, and chemical state of each component. New approaches can be devised in the near future to characterize Cu-based WGSR catalysts using the kinetic strategy described herein. Moreover, it is worth noting that the TOF of the WGSR over CZA must be estimated using the intrinsic TOF of the catalytic cycle. The rate of the cycle in the WGSR corresponds to that of the Cu^0/Cu^+ oxidation. The rate should be the $k_f P_{H2O}^{0.5}$ term in Eq. (5). In the case of a typical reformed gas composition, the reactant gas contains 30 % steam at 30.4 kPa under atmospheric pressure. The intrinsic reaction rate can be calculated using Eq. (5) as 0.161 mol/h g-cat, and the selectivity in the reduction step is 0.494 (selectivity to CO_2 formation), with P_{CO} and P_{H2} being 10.1 and 55.7 kPa, respectively (Table 3).

3.4. Estimation of number of active sites

The pulse experiment data also assisted in determining the number of active sites on the CZA catalysts. The average amount of H_2 formed can be used to estimate the number of oxidized Cu^0 sites. The formation of one H_2 molecule indicates that two Cu^0 sites were oxidized to Cu^+. Notably, the number of oxidized Cu^0 sites with H_2O obtained in the pulse experiments probably depended on the pulse reaction temperature. The number of active sites, the bulk Cu content evaluated by XRF analysis, and the surface Cu^0 estimated using the N_2O titration method are listed in Table 7. It is worth noting that the number of active sites was significantly lower than the number of surface Cu^0 atoms, with only 23.5 % of the surface Cu^0 atoms being active sites. Fichtl et al. reported that N_2O titration can help in estimating not only the number of surface

Table 7
Number of active sites and surface-exposed Cu^0 atoms.

Cu content[a] (mmol/g-cat)	Surface Cu^0[b] (μmol/g-cat)	Active Cu^0[c] (μmol/g-cat)
6.38	272	63.8
100 %	4.26 %	1.00 %

[a] Measured by XRF.
[b] Estimated by N_2O titration.
[c] Evaluated through the H_2O pulse experiments.

copper atoms, but also the oxygen defects located at the copper–zinc interface [31]. The difference between the amount of surface Cu^0 estimated by N_2O titration and the number of active sites for H_2O in this study might be due to oxygen defects. The TOF of the CZA catalyst can be recalculated using the obtained number of active sites (63.8 μmol/g-cat) and the aforementioned intrinsic reaction rate (0.161 mol/h g-cat). The TOF of the assumed rate-determining oxidation step was estimated to be 0.701 s^{-1}. The effective TOF for CO_2 formation, which is the TOF of the CO oxidation ($Cu_2O + CO \rightarrow 2Cu^0 + CO_2$) and is often analyzed in WGSR-related studies, was found to be 0.346 s^{-1}. The TOF is strongly affected by not only the gas composition, but also the estimation of the active sites. It is worth noting that not all the surface Cu^0 atoms functioned as active sites. In this study, almost one-fourth of the surface Cu^0 atoms (23.5 %) likely functioned as active sites for the WGSR. These results indicate that the presence of H_2 could suppress the efficiency of the reduction step. The rate of the redox cycle, that is, the rate of the H_2O-induced oxidation of Cu^0 to Cu^+ ($Cu^0 + H_2O \rightarrow \frac{1}{2}Cu_2O + H_2$) was unaffected by the presence of a significant amount of H_2.

4. Conclusions

A simple rate equation based on a competitive redox mechanism is proposed for the low-temperature WGSR in a reformed gas atmosphere. Under a reductive atmosphere in the presence of hydrogen, the rate-determining step was assumed to be the H_2O-enabled oxidation of Cu^0 to Cu^+, which produced H_2. The presence of abundant H_2 affected the CO conversion rate because H_2 reduced Cu^+ to Cu^0 without consuming CO. The rate constant k_f and selectivity factor κ are important parameters of the proposed rate equation for understanding catalytic behavior. The rate constant k_f determines the rate of the catalytic cycle of the WGSR, and the selectivity factor κ possibly controls CO conversion selectivity. Successive pulse experiments can be used to evaluate the number of active sites on CZA catalysts for low-temperature WGSR. Almost 1 at% of the Cu in the CZA catalyst exhibited activity for the WGSR, which corresponded to 23.5 % of the surface Cu^0 atoms.

In this study, the WGSR conducted over CZA catalysts in a reformed gas atmosphere was found to be affected by the selectivity of competitive reduction of Cu^+ by H_2 or CO. Our findings can help to improve the catalyst design for high-performance Cu-based catalysts. Particularly, suppressing the reduction of Cu^+ by H_2 is expected to facilitate the creation of high-performance catalysts.

The rate equation proposed in this study is specific to practical WGSR over Cu-based catalysts in a reformed gas atmosphere. Because this rate equation is intended for use under competitive reduction, the current form of the equation is not applicable to WGSR conditions wherein H_2 is absent. Additionally, the effects of CO_2 and reaction temperature on this equation have not been comprehensively discussed. Further studies are necessary to extend the proposed rate equation to include these effects.

CRediT authorship contribution statement

Keita Taniya: Visualization, Writing – original draft, Writing – review & editing, Supervision. **Yasuhiro Horie:** Methodology, Formal analysis, Investigation. **Ryo Fujita:** Formal analysis, Investigation. **Yuichi Ichihashi:** Writing – review & editing. **Satoru Nishiyama:** Conceptualization, Writing – original draft, Writing – review & editing, Supervision, Project administration.

Declaration of Competing Interest

The authors declare that they have no known competing financial interests or personal relationships that could have appeared to influence the work reported in this paper.

Data Availability

The data that has been used is confidential.

Acknowledgements

We would like to thank Editage (www.editage.com) for English language editing.

Appendix A. Supporting information

Supplementary data associated with this article can be found in the online version at doi:10.1016/j.apcatb.2023.122568.

References

[1] M.J.L. Ginés, N. Amadeo, M. Laborde, C.R. Apesteguía, Activity and structure-sensitivity of the water-gas shift reaction over CuZnAl mixed oxide catalysts, Appl. Catal. A: Gen. 131 (1995) 283–296, https://doi.org/10.1016/0926-860X(95)00146-8.

[2] T. Shishido, M. Yamamoto, I. Atake, D. Li, Y. Tian, H. Morioka, M. Honda, T. Sano, K. Takehira, Cu/Zn-based catalysts improved by adding magnesium for water–gas shift reaction, J. Mol. Catal. A: Chem. 253 (2006) 270–278, https://doi.org/10.1016/j.molcata.2006.03.049.

[3] Y. Choi, H.G. Stenger, Water gas shift reaction kinetics and reactor modeling for fuel cell grade hydrogen, J. Power Sources 124 (2003) 432–439, https://doi.org/10.1016/S0378-7753(03)00614-1.

[4] R.J. Byron Smith, M. Longanathan, M.S. Shantha, A review of the water gas shift reaction kinetics, Int. J. Chem. React. Eng. 8 (2010), https://doi.org/10.2202/1542-6580.2238.

[5] T.M. Yurieva, G.K. Boreskov, V. Sh. Gruver, Nature of the catalytically active component of copper–chromium catalysts for the conversion of carbon monoxide, Kinet. Katal. 10 (1969) 294–300.

[6] T. van Herwijnen, W.A. de Jong, Kinetics and mechanism of the CO shift on CuZnO: 1. Kinetics of the forward and reverse CO shift reactions, J. Catal. 63 (1980) 83–93, https://doi.org/10.1016/0021-9517(80)90061-5.

[7] T. Takagawa, G. Pleizer, Y. Amenomiya, Methanol synthesis from $CO_2 + H_2$ I. characterization of catalysts by TPD, Appl. Catal. 18 (1985) 285–293, https://doi.org/10.1016/S0166-9834(00)84007-5.

[8] C.T. Campbell, K.A. Daube, A surface science investigation of the water-gas shift reaction on Cu(111), J. Catal. 104 (1987) 109–119, https://doi.org/10.1016/0021-9517(87)90341-1.

[9] T. Salmi, R. Hakkarainer, Kinetic study of the low-temperature water-gas shift reaction over a Cu—ZnO catalyst, Appl. Catal. 49 (1989) 285–306, https://doi.org/10.1016/S0166-9834(00)83024-9.

[10] E.G.M. Kuijpers, R.B. Tjepkema, W.J.J. van der Wal, C.M.A.M. Mesters, S.F.G. M. Spronck, J.W. Geus, Appl. Catal. 25 (1986) 139–147, https://doi.org/10.1016/S0166-9834(00)81230-0.

[11] J. Nakamura, J.M. Cambell, C.T. Campbell, Kinetics and mechanism of the water-gas shift reaction catalysed by the clean and Cs-promoted Cu(110) surface: a comparison with Cu(111), J. Chem. Soc. Faraday Trans. 86 (1990) 2725–2734, https://doi.org/10.1039/FT9908602725.

[12] R.A. Hadden, Vandervell, K.C. Waugh, G. Webb, Proceedings: 9th International Congress on Catalysis, Calgary, vol. 4, 1988, 1835.

[13] S. Fujita, M. Usui, N. Takezawa, Mechanism of the reverse water gas shift reaction over Cu/ZnO catalyst, J. Catal. 134 (1992) 220–225, https://doi.org/10.1016/0021-9517(92)90223-5.

[14] C.V. Ovesen, P. Stoltze, J.K. Norksov, C.T. Campbell, A kinetic model of the water gas shift reaction, J. Catal. 134 (1992) 445–468, https://doi.org/10.1016/0021-9517(92)90334-E.

[15] F.H.M.P. Habraken, G.A. Bootsma, The kinetics of the interactions of O_2 and N_20 with a Cu(110) surface and of the reaction of CO with adsorbed oxygen studied by means of ellipsometry, AES and LEED, Surf. Sci. 87 (1979) 333–347, https://doi.org/10.1016/0039-6028(79)90533-8.

[16] O.P. Van Pruissen, M.M.M. Dings, O.L.J. Gijzeman, Surface and subsurface oxygen on Cu(111), Cu(111)-Fe and Cu(110) and their influence on the reduction with CO and H_2, Surf. Sci. 179 (1987) 377–386, https://doi.org/10.1016/0039-6028(87)90064-1.

[17] G.C. Chinchen, M.S. Spencer, K.C. Waugh, D.A. Whan, Promotion of methanol synthesis and the water-gas shift reactions by adsorbed oxygen on supported copper catalysts, J. Chem. Soc. Faraday Trans. 83 (1987) 2193–2212, https://doi.org/10.1039/F19878302193 (1).

[18] M.J.L. Ginés, N. Amadeo, M. Laborde, C.R. Apesteguía, Activity and structure-sensitivity of the water-gas shift reaction over Cu–Zn–Al mixed oxide catalysts, Appl. Catal. A 131 (1995) 283–296, https://doi.org/10.1016/0926-860X(95)00146-8.

[19] A.A. Gokhale, J.A. Dumesic, M. Mavrikakis, On the mechanism of low-temperature water gas shift reaction on copper, J. Am. Chem. Soc. 130 (2008) 1402–1414, https://doi.org/10.1021/ja0768237.

[20] C.M. Kalamaras, P. Panagiotopoulou, D.I. Kondarides, A.M. Efstathiou, Kinetic and mechanistic studies of the water–gas shift reaction on Pt/TiO_2 catalyst, J. Catal. 264 (2009) 117–129, https://doi.org/10.1016/j.jcat.2009.03.002.
[21] N.A. Koryabkina, A.A. Phatak, W.F. Ruettinger, R.J. Farrauto, F.H. Ribeiro, Determination of kinetic parameters for the water–gas shift reaction on copper catalysts under realistic conditions for fuel cell applications, J. Catal. 217 (2003) 233–239, https://doi.org/10.1016/S0021-9517(03)00050-2.
[22] N.M.B. Oliveira, G.P. Valenca, R. Vieira, Water gas shift reaction on copper catalysts supported on alumina and carbon nanofibers, Chem. Eng. Trans. 43 (2015) 931–936, https://doi.org/10.3303/CET1543156.
[23] Y. Li, Q. Fu, M. Flytzani-Stephanopoulos, Low-temperature water-gas shift reaction over Cu- and Ni-loaded cerium oxide catalysts, Appl. Catal. B 27 (2000) 179–191, https://doi.org/10.1016/S0926-3373(00)00147-8.
[24] D.C. Yeragi, N.C. Pradhan, A.K. Dalai, Low-temperature water-gas shift reaction over Mn-promoted Cu/Al_2O_3 catalysts, Catal. Lett. 112 (2006) 139–148, https://doi.org/10.1007/s10562-006-0193-9.
[25] J.Y. Kim, J.A. Rodriguez, J.C. Hanson, A.I. Frenkel, P.L. Lee, Reduction of CuO and Cu_2O with H_2: H embedding and kinetic effects in the formation of suboxides, J. Am. Chem. Soc. 125 (2003) 10684–10692, https://doi.org/10.1021/ja0301673.
[26] J.A. Rodriguez, J.Y. Kim, J.C. Hanson, M. Pérez, A.I. Frenkel, Reduction of CuO in H_2: in situ time-resolved XRD studies, Catal. Lett. 85 (2003) 247–254, https://doi.org/10.1023/a:1022110200942.
[27] X. Wang, J.C. Hanson, A.I. Frenkel, J.-Y. Kim, J.A. Rodriguez, Time-resolved studies for the mechanism of reduction of copper oxides with carbon monoxide: complex behavior of lattice oxygen and the formation of suboxides, J. Phys. Chem. B 108 (2004) 13667–13673, https://doi.org/10.1021/jp040366o.
[28] H.Y. Huang, J. Padin, R.T. Yang, Comparison of π-complexations of ethylene and carbon monoxide with Cu^+ and Ag^+, Ind. Eng. Chem. Res. 38 (1999) 2720–2725, https://doi.org/10.1021/ie990035b.
[29] Y. Yin, P. Tan, X.-Q. Liu, J. Zhu, L.-B. Sun, Constructing a confined space in silica nanopores: an ideal platform for the formation and dispersion of cuprous sites, J. Mater. Chem. A 2 (2014) 3399–3406, https://doi.org/10.1039/C3TA14760F.
[30] J. Sárkány, J.L. d'Itri, W.M.H. Sachtler, Redox chemistry in excessively ion-exchanged Cu/Na-ZSM-5, Catal. Lett. 16 (1992) 241–249, https://doi.org/10.1007/BF00764336.
[31] M.B. Fichtl, J. Schumann, I. Kasatkin, N. Jacobsen, M. Behrens, R. Schlögl, M. Muhler, O. Hinrichsen, Counting of oxygen defects versus metal surface sites in methanol synthesis catalysts by different probe molecules, Angew. Chem. 126 (2014) 7163–7167, https://doi.org/10.1002/ange.201400575.